AGU ADVANCING EARTH AND SPACE SCIENCE

Water Resources Research

RESEARCH ARTICLE
10.1029/2021WR031020

In-Situ Quantification and Prediction of Water Yield From Southern US Pine Forests

Subodh Acharya[1], David A. Kaplan[2], Daniel L. McLaughlin[3], and Matthew J. Cohen[1]

[1]School of Forest, Fisheries and Geomatics Sciences, University of Florida, Gainesville, FL, USA, [2]Environmental Engineering Sciences Department, University of Florida, Gainesville, FL, USA, [3]Department of Forest Resources and Conservation, Virginia Tech, Blacksburg, VA, USA

Key Points:

- We quantified soil evapotranspiration (ET) and interception using high frequency time series of soil moisture profiles
- Water yield (precipitation minus ET) was well predicted by a model based on aridity, water table depth, and leaf area index
- Forest management can meaningfully influence regional water supply planning in the US southeastern coastal plain

Supporting Information:

Supporting Information may be found in the online version of this article.

Correspondence to:

M. J. Cohen,
mjc@ufl.edu

Citation:

Acharya, S., Kaplan, D. A., McLaughlin, D. L., & Cohen, M. J. (2022). *In-situ* quantification and prediction of water yield from southern US pine forests. *Water Resources Research*, *58*, e2021WR031020. https://doi.org/10.1029/2021WR031020

Received 9 AUG 2021
Accepted 14 APR 2022

Author Contributions:

Conceptualization: Subodh Acharya, David A. Kaplan, Daniel L. McLaughlin, Matthew J. Cohen
Data curation: Subodh Acharya, Matthew J. Cohen
Formal analysis: Subodh Acharya, David A. Kaplan, Daniel L. McLaughlin, Matthew J. Cohen
Funding acquisition: David A. Kaplan, Daniel L. McLaughlin, Matthew J. Cohen
Investigation: Subodh Acharya
Methodology: Subodh Acharya, David A. Kaplan, Daniel L. McLaughlin, Matthew J. Cohen
Project Administration: David A. Kaplan, Daniel L. McLaughlin, Matthew J. Cohen
Software: Subodh Acharya
Supervision: David A. Kaplan, Daniel L. McLaughlin, Matthew J. Cohen

Abstract Forest management can play an important role in landscape-scale water balances and thus regional water supply planning, necessitating improved quantification and prediction of forest water yield (i.e., rainfall minus evapotranspiration (ET)). We used high frequency soil moisture data to quantify soil ET and interception in 30 pine stands capturing regional variation in aridity, hydrogeology, and forest management. We evaluated typical forest rotation stages (i.e., clear cuts through mature stands), as well as stands restored to historical, lower biomass conditions. Our results supported the expectation that forest management can strongly influence local water yield. A simple model using leaf area index (LAI), hydrogeologic setting, and climate aridity (P:ET) explained nearly 80% of observed water yield variation. LAI emerged as the dominant forest structural control, influencing both soil ET and interception rates, with each unit decrease in LAI increasing water yield by nearly 10 cm. While other forest attributes (e.g., basal area, groundcover, species) were less important for predicting stand-level water balances, aridity and hydrogeologic setting emerged as highly significant predictors of water yield. We further observed small and short-lived effects of low-intensity prescribed fires on soil ET and no discernible effect of pine species, suggesting that maintaining low density pine forests—regardless of species—is a viable management strategy for increasing water yield. Overall, our results illustrate the utility of soil moisture-based methods for stand-level water balances and provide useful models for predicting landscape water yield under a range of forest management and hydroclimatic settings now and in the future.

Plain Language Summary Evapotranspiration is a major part of the water balance in coastal plain forests. In this work we use soil moisture measurements to calculate how much water forests use, and thus how much is left over for aquifer recharge and stream flow generation. We show that this "water yield" is accurately predicted using local climate, hydrogeology, and forest density (using leaf area index). Since water supply planning depends on how much water yield occurs from the landscape, our simple models to predict water yield can be used to understand how forest management decisions impact water supply, and inform how incentives to forest landowners can help meet regional water supply sustainability goals.

1. Introduction

Forests make up 31% of global land cover (Keenan et al., 2015) and exert a primary control on terrestrial and atmospheric water fluxes (Bonan, 2008; Fisher et al., 2009; Makarieva et al., 2013) by affecting the partitioning of precipitation into evapotranspiration (ET), infiltration, and runoff (Good et al., 2015; D. M. Lawrence et al., 2007; Mercado-Bettín et al., 2017). Decades of previous research have shown strong associations between plant community structure and rainfall partitioning (e.g., reviews in J. A. Jones et al., 2020; Komatsu & Kume, 2020; Zhang et al., 2017). Broadly, forest biomass reductions increase local water yield (defined as precipitation minus ET) by reducing interception and transpiration, which are dominant components of the total ET flux (e.g., Bosch & Hewlett, 1982; Cecílio et al., 2019; Davie & Fahey, 2018; Peña-Arancibia et al., 2019; Schulze & George, 1987; Sun, Zuo, et al., 2008). By complement, afforestation is associated with reduced water yield in catchments globally, especially in arid regions (Brown et al., 2005; Farley et al., 2005; Filoso et al., 2017). While it is important to consider regional effects of reducing local ET on downwind rainfall (Creed et al., 2019; Stickler et al., 2013), the clear local linkages between forest cover and water yield imply an opportunity to manage forests for water yield benefits to human uses and environmental flows (Greenwood et al., 2008; McLaughlin et al., 2013).

Validation: Subodh Acharya
Visualization: Subodh Acharya, David A. Kaplan, Daniel L. McLaughlin
Writing – original draft: Subodh Acharya, David A. Kaplan, Daniel L. McLaughlin, Matthew J. Cohen
Writing – review & editing: Subodh Acharya, David A. Kaplan, Daniel L. McLaughlin, Matthew J. Cohen

Globally, forests are managed for a diversity of functions and ecosystem services (García-Nieto et al., 2013), from provisioning of timber and other wood products (Duncker et al., 2012), to carbon sequestration and other climate change mitigation (Bell & Lovelock, 2013; Lutz et al., 2016), to habitat value and fire regime maintenance (Freeman et al., 2017; Hunter, 1990; Stephens et al., 2013). In many regions, including the southeastern United States, a large fraction of forested lands are intensively managed for timber production (Dudley et al., 2014; Sohngen et al., 1999; Trømborg et al., 2000), with high-density, monotypic, short-rotation plantings, and management actions ranging from clearcutting and thinning to competition control and fertilization (Becknell et al., 2015; McLaughlin et al., 2013). Managing the biomass in these forests may afford opportunities to optimize tradeoffs among wood products, water yield, and other services (González-Sanchis et al., 2019; C. N. Jones et al., 2018). However, while incentive and payment-for-ecosystem-services (PES) programs have been developed to support carbon sequestration (Jayachandran et al., 2017), habitat provisioning (Tuanmu et al., 2016), and water quality protection (Kreye et al., 2014) in forests, efforts to optimize water quantity (e.g., hydrological easements or "payment for water yield" programs) have been slower to develop (Susaeta et al., 2017). This lag is due, at least in part, to uncertainties about the relationships among forest structure, climate variation, and dynamic water yield (McNulty et al., 2018).

Most studies relating forest cover to water yield are performed at the watershed scale, using flow data from the basin outlet (i.e., the "hydrometric method" (Bosch & Hewlett, 1982)) and are thus most informative regarding hydrologic effects of basin-scale, rather than stand-scale, changes. Moreover, most analyses focus on complete timber harvest (Rothacher, 1970; Stednick, 1996) or wholesale deforestation or afforestation (Farley et al., 2005; Sahin & Hall, 1996; Zhang et al., 2017), though forest thinning has been explicitly studied in some systems (Downing, 2015; Hawthorne et al., 2013; Lesch & Scott, 1997; Yurtseven et al., 2018). Even when adequately controlled using a paired watershed approach (e.g., Brown et al., 2005; Hornbeck et al., 1997), the outcomes of these analyses are difficult to use for direct predictions of how stand-scale management of forest structure (e.g., motivated by PES incentive programs) would manifest as local water yield, limiting their widespread utility. For example, while confirming the overall direction and average strength of water yield changes with forest cover reduction, Bosch and Hewlett (1982) explicitly note that extreme variation in outcomes across "such a scattered set of experimental catchments" prevents generalizable statistical inference and development of "derived functions relating water-yield changes to forestry practices".

An important limitation of the watershed-scale approaches described above is thus limited support for local decisions about wood versus water tradeoffs without additional empirical data collection. Specifically, measurements of forest ET and resulting water yield over regional gradients in environmental setting (e.g., soil types, hydrogeology) and across a diversity of operationally relevant management regimes (i.e., conservation vs. production forestry (Becknell et al., 2015)) are required in order to adequately define this trade-off (Schwaiger et al., 2019). Using the paired watershed approach at this scale of inquiry is unfeasible given the need to identify, treat, and monitor a large number of treatment and control watersheds; treatment costs alone make this endeavor impractical at the watershed scale (Bosch & Hewlett, 1982). Forest ET at the stand scale can be directly measured using the eddy covariance method (Paul-Limoges et al., 2020; Soubie et al., 2016; Sun, Noormets, et al., 2008), making it a potentially useful approach. However, installation and maintenance of eddy covariance towers at the granularity required is prohibitively expensive (e.g., Markwitz & Siebicke, 2019), highlighting the need for lower-cost methods to measure forest water use and yield at a large number of sites in support of accurate and regionally appropriate relationships between forest structure and water yield.

Within this context, the overarching goal of our work was to quantify changes in water yield induced by differing management strategies in pine forests of the southeastern United States, a region of increasing water shortages (e.g., Sun, 2013). To do so, we applied a soil moisture-based method for measuring soil evaporation and transpiration (Nachabe et al., 2005), coupled with a recently developed, parallel method to estimate interception (Acharya et al., 2020) to quantify the total ET flux and resulting water yield in 30 experimental plots distributed across five sites in Florida (USA) (Figure 1). Sites were selected to span gradients in climate, hydrogeological setting, and soil types. Within sites, experimental plots characterized a wide range of forest structural attributes (from clearcuts to mature pine plantations) and management approaches (e.g., species selection and restoration activities, including fire), with the overarching hypothesis that lower biomass stands would yield more water. Using these direct empirical measurements of stand water balances, we then sought to develop simple operational models of water yield based on readily measurable site properties (e.g., forest stand attributes, hydroclimate conditions, and

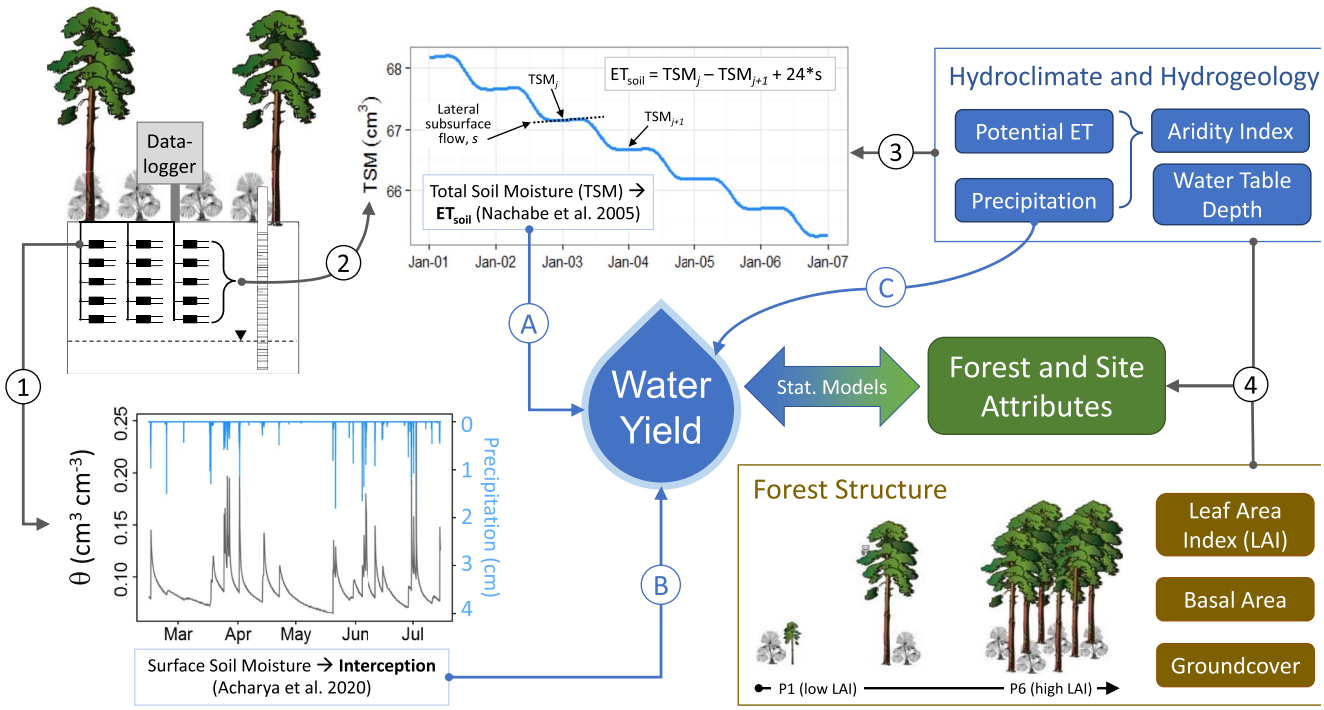

Figure 1. Water yield (Y_w) estimates are obtained by subtracting (a) soil evapotranspiration losses (ET_{soil}) and (b) interception from (c) precipitation. Data flows supporting these calculations include: time series of surface soil moisture during storm events (a) to estimate interception; time series of depth-integrated total soil moisture (b) and hydroclimate data (c) to estimate ET_{soil}; and site attributes (aridity, water table depth) and forest structure (leaf area index, basal area, ground cover) variables (d) used in statistical predictions of Y_w. Maps and photographs of selected study sites are presented in Supporting Information S1.

hydrogeologic setting) that allow for robust predictions of water yield in new settings and under alternative future climate and land management scenarios.

2. Materials and Methods

2.1. Study Sites

We selected five study sites (Econfina – EF, Little River – LR, Deer Haven – DH, Green Swamp – GS, and Longleaf Flatwoods – LF) across Florida, USA, each with six 2-ha plots spanning a range of forest structural characteristics (Table 1; Figure S1 in Supporting Information S1). Sites varied in hydroclimatic forcing, with aridity index (i.e., precipitation: potential ET (PET)) during our study period (2014–2017) ranging from 0.96 to 1.07. Geologic setting also varied across sites, with two sites having all or some plots located in unconfined aquifer settings with deep (>5 m) water table (WT) depths (4 of 6 plots at site EF; all 6 plots at site LR). In contrast, at plots where the regional aquifer is confined by a shallow aquiclude, mean WT depths ranged from near ground surface to a maximum of 2 m belowground. Soils were uniformly dominated by fine sand, consisting of deep well-drained entisols (Lakeland and Penney sands) and ultisols (the Blanton-Alpin-Bonneau complex), moderately drained soils (Tavares and Milhopper sands), and more poorly drained spodosols typical of Florida's flatwoods (Plummer, Sparr, Pomona, Ona, Chipley, Pottsburg, and Newnan sands). We selected six plots within each site to capture a wide range of forest structural attributes and forest management strategies. Each site contained both a recent clear-cut with low leaf area index (LAI) and a mature pine stand with high LAI and basal area (BA) (Table 1). Remaining plots at each site had intermediate LAI and BA values due to rotation age and varying midstory management and canopy thinning. Plots also varied in pine species, including slash pine (*Pinus elliottii*), sand pine (*Pinus clausa*), and loblolly pine (*Pinus taeda*), and understory composition and cover (hereafter ground cover (GC)). A subset plots ($n = 7$) underwent low-intensity, prescribed fire during the study, allowing us to assess short-term fire effects on water yield using pre- and post-fire data.

Table 1
Summary of Plot Attributes Across Five Sites Showing Longitude (Long.), Latitude (Lat), Mean (and Standard Deviation) of Annual Rainfall, Potential Evapotranspiration and Water Table Depth

Plot	Long.	Lat.	Rainfall (cm)	PET (cm)	WT (m)	Spp	LAI	BA	I_a (cm)	Yw (cm)
DH1	−82.3375	29.7458	130 (18)	132 (5)	−0.82 (0.5)	PT	0.75	0	26.4	33.8 (4.1 - 54.6)
DH2	−82.3281	29.7639	130 (18)	132 (5)	−0.94 (0.5)	PE	2.47	23.4	32.2	29.9 (−5.8 - 51.8)
DH3	−82.3808	29.7789	130 (18)	132 (5)	−0.58 (0.4)	PE	1.40	18.5	28.1	26.0 (−2.7 - 45.6)
DH4	−82.3875	29.7494	130 (18)	132 (5)	−0.97 (0.5)	PE	3.48	27.0	28.9	22.6 (−8.1 - 42.6)
DH5	−82.3894	29.7494	130 (18)	132 (5)	−0.59 (0.3)	PT	3.76	51.3	28.1	25.0 (−8.2 - 46.9)
DH6	−82.3364	29.7656	130 (18)	132 (5)	−1.32 (0.7)	PE	3.65	23.8	32.8	10.1 (−18.8 - 30.3)
EF1	−85.6153	30.4000	153 (15)	144 (11)	−5.48 (0.9)	C	0.12	0	21.2	97.8 (81.5 - 114.5)
EF2	−85.6139	30.3947	153 (15)	144 (11)	−0.59 (0.3)	PE	1.05	29.5	19.6	74.6 (59.6 - 93.2)
EF3	−85.6150	30.3975	153 (15)	144 (11)	−5.48 (0.9)	PC	2.41	39.6	21.4	72.4 (57.7 - 87.1)
EF4[a]	−85.6139	30.3964	153 (15)	144 (11)	−1.34 (0.4)	PE	0.65	13.0	18.8	93.3 (83.8 - 107.6)
EF5	−85.6150	30.3989	153 (15)	144 (11)	−5.48 (0.9)	PC	0.82	10.8	19.8	83.0 (62.5 - 98.5)
EF6[a]	−85.6117	30.4314	153 (15)	144 (11)	−5.48 (0.9)	PP	0.51	4.4	21.4	74.9 (55.2 - 90.8)
GS1	−82.0992	28.4000	131 (10)	143 (3)	−1.85 (0.3)	C	1.07	0	31.6	50.8 (44.3 - 61.1)
GS2	−82.0950	28.4081	131 (10)	143 (3)	−0.83 (0.4)	PE	2.56	36.0	31.1	25.4 (17.8 - 35.8)
GS3[a]	−82.1000	28.4056	131 (10)	143 (3)	−0.98 (0.6)	PE	2.04	29.4	31.6	20.3 (17.5 - 27.9)
GS4[a]	−82.0964	28.4008	131 (10)	143 (3)	−0.95 (0.4)	PE	1.12	18.4	27.1	34.8 (23.0 - 44.5)
GS5[a]	−82.0978	28.4008	131 (10)	143 (3)	−0.68 (0.4)	PE	1.13	12.8	30.4	30.1 (18.7 - 41.7)
GS6	−82.1050	28.4067	131 (10)	143 (3)	−1.46 (0.7)	PP	0.50	3.8	27.0	43.9 (36.4 - 51.1)
LF1	−82.2219	29.5364	134 (16)	136 (4)	−0.6 (0.4)	C	0.26	0	26.4	45.3 (31.0 - 79.5)
LF2	−82.2225	29.5356	134 (16)	136 (4)	−0.70 (0.5)	PE	2.85	38.7	29.4	29.1 (10.0 - 44.1)
LF3	−82.2239	29.5361	134 (16)	136 (4)	−0.63 (0.4)	PE	1.23	16.3	31.1	44.3 (27.4 - 73.6)
LF4	−82.2225	29.5353	134 (16)	136 (4)	−0.63 (0.5)	PE	0.86	13.4	32.8	44.4 (29.2 - 72.0)
LF5[a]	−82.1995	29.5697	134 (16)	136 (4)	−2.86 (0.6)	PE	2.72	23.9	33.3	25.0 (3.1 - 53.1)
LF6[a]	−82.2031	29.5672	134 (16)	136 (4)	−2.36 (0.4)	PP	0.93	8.5	33.2	46.8 (34.2 - 71.9)
LR1	−82.9819	30.0269	144 (20)	136 (4)	−7.76 (1.1)	C	0.46	0	22.8	65.0 (38.7 - 80.7)
LR2	−82.9994	29.9994	144 (20)	136 (4)	−7.76 (1.1)	PE	3.08	48.1	30.5	55.2 (25.6 - 71.0)
LR3	−82.9919	30.0322	144 (20)	136 (4)	−7.76 (1.1)	PE	0.80	4.8	18.3	58.2 (31.3 - 92.9)
LR4	−82.9925	30.0289	144 (20)	136 (4)	−7.76 (1.1)	PE	2.48	15.5	23.2	75.7 (45.9 - 90.8)
LR5	−82.9819	30.0256	144 (20)	136 (4)	−7.76 (1.1)	PE	1.50	13.5	22.8	54.4 (28.7 - 74.5)
LR6	−83.0083	30.0342	144 (20)	136 (4)	−7.76 (1.1)	PP	1.22	9.3	17.8	65.4 (29.8 - 88.2)

Note. Dominant species (C – clearcut, PC – *Pinus clausa*, PE – *Pinus elliottii*, PP – *Pinus palustris*, PT – *Pinus taeda*), site leaf area index (LAI, unitless) and basal area (BA, $m^2\ ha^{-1}$) are provided, along with average interception losses (I_a) and the site mean (and range) of annual water yield (Y_w). Note that clearcut sites (Spp. = C) had sufficient canopy > 1 m to measure LAI, but no trees with diameter at breast height >5 cm to measure BA.

[a]Sites at which prescribed fires occurred during the project duration.

2.2. Forest Attributes

At each plot, we measured BA ($m^2\ ha^{-1}$), leaf area index (LAI, $m^2\ m^{-2}$) and GC to assess their influence on forest ET and thus water yield. Basal area was measured at the outset of the study using the point-centered quarter method. To capture seasonal patterns and annual changes, LAI and GC were measured quarterly in a 5 × 5 m grid covering 0.25 ha centered on plot instrumentation (see below), yielding 121 observations per plot. We measured LAI, capturing both midstory and canopy, using a plant canopy analyzer (LAI-2200C, LI-COR, Lincoln, Nebraska) at 1-m above the ground surface. We used a 90° restricting cap to ensure that measurements were made facing north and obtained during the middle (10 a.m.–2 p.m.) of each sampling day. We used raw projected (i.e., one-sided) LAI observations corrected to account for the non-random orientation of pine needles, which results

in LAI underestimation by 12% when using the LI-COR LAI-2000 (Stenberg et al., 1994; Weiss et al., 2004); specifically, final projected LAI values are raw observed values multiplied by 0.88. At the same locations, GC (%) was recorded visually in 1-m^2 quadrats.

2.3. Field Instrumentation

Each plot was instrumented to collect high frequency soil moisture data at multiple soil depths in three locations selected to capture variation in canopy and understory cover; at clear cut sites, groundcover alone guided location selection. At each location (3 per plot), time domain reflectometry soil moisture sensors (CS655, Campbell Scientific, Logan, UT) were installed in the side wall of an augered hole at depths 0.15, 0.3, 0.5, 0.8, and 1.5 m belowground. At unconfined (i.e., deep WT) plots, an additional sensor was installed at 2.5 m depth. These depths were selected to capture dynamic soil moisture variation in shallower soil profiles and establish a high-moisture, low-variation bottom boundary to meet the assumptions of the Nachabe et al. (2005) method; we present evidence that validates this assumption in the supplemental information (Figures S4, S5, and S6 in Supporting Information S1). Holes were backfilled with augered soil, attempting to match soil layering and bulk density. Each sensor was configured to record volumetric soil moisture content (θ) at 15-min intervals, and data were collected from 2014 to 2017 using CR800 data loggers (Campbell Scientific, Logan, UT). At each confined (i.e., shallow WT) plot, we also installed a WT monitoring well (2-cm, screened PVC well) 2–3 m belowground. Total pressure transducers (HOBO U20L-04, Onset Computer Corp., Bourne, MA) and an additional barometric pressure transducer (same model) installed in a dry well (McLaughlin & Cohen, 2011) were used to measure 15-min water levels relative to the ground surface. At unconfined sites, we deployed pressure transducers in one pre-existing deep groundwater well per site. A weather station was installed in the clear-cut plot of each site to collect meteorological data (CM106B tripod, CM206 cross-arm, TE525-L25 tipping bucket rain gage at 1 m above ground, CS300-L14 pyranometer at 2 m above ground, 03002-L14 anemometer/wind vane at 2 m above ground, HMP60-L8 relative humidity probe at 2 m above ground) every 3 s, which were then used to calculate mean values at 15-min intervals. Weather data were used to estimate daily PET with the Penman (1948) method, which was selected to avoid assumptions about stomatal conductance parameters required in the Penman-Monteith formulation. When comparing results between the two PET estimates, we found nearly identical values and across-site patterns.

2.4. Soil Water Evapotranspiration Estimates (ET_{soil})

Here, we distinguish between soil water ET (i.e., vadose and groundwater uptake via evaporation and transpiration) and interception (and subsequent evaporation), which together represent total ET (Miralles et al., 2020). Soil water ET (hereafter ET_{soil}) was estimated from 15-min soil moisture data using a method developed by (Nachabe et al., 2005) (Figure 1a). Compared to the WT-based method (Gribovszki et al., 2008; Loheide, 2008) pioneered by White (1932), advantages of this soil moisture-based approach are twofold: (a) it includes both groundwater and vadose zone water uptake; and (b) it does not require specific yield (S_y), eliminating uncertainty in ET estimation originating from this parameterization. Although the original method (Nachabe et al., 2005) was developed and applied in a shallow WT environment, use in regions with deeper water tables is possible, in principle, provided that soil moisture dynamics of the root-zone are captured. We validate this assumption in the supplemental information (Section S3 in Supporting Information S1), showing that soil moisture measured at our deepest sensors was uniformly much higher (~2x) and much less variable (by 80%) than throughout the rest of the vadose zone, suggesting that nearly all soil moisture variation (and thus water use) occurs within shallower soil profiles. We note that our study sites are dominated by fine sand such that soil moisture profiles quickly reach hydrostatic equilibrium; slower equilibration may limit application in finer textured soils.

Following the Nachabe et al. (2005) method, we computed the integral of soil moisture volume through the soil profile (i.e., total soil moisture; TSM) for each location (three per plot) using trapezoidal integration of 15-min observations collected by the 5 (or 6) soil moisture sensors:

$$\mathrm{TSM} = \sum_{i=1}^{n-1} \frac{1}{2} * (\theta_i + \theta_{i+1})(z_i - z_{i+1}) + \theta_1 * z_1 \quad (1)$$

where z is depth below ground surface for each sensor and θ_i is the soil moisture content observed at sensor i. The last term on the right side of Equation 1 ($\theta_1 * z_1$) accounts for soil moisture above the first sensor to the ground surface. Daily ET_{soil} (for non-precipitation days) for each plot location was then estimated as:

$$ET_{soil} = TSM_t - TSM_{t+1} + 24 * s \quad (2)$$

where TSM_t and TSM_{t+1} are total soil moisture at midnight on day t and t+1, respectively. Assuming ET is negligible at night, s is hourly soil moisture recovery due to vertical or lateral soil water redistribution to the sensor location (induced by the gradient developed by daytime root water uptake), determined from the mean nighttime TSM slope between 11:00 p.m. to 6:00 a.m. for nights t and t+1. Daily ET_{soil} estimates from the three locations were averaged to yield plot-level ET_{soil} time series. As with the White (1932) method, this approach is not applicable during precipitation events, limiting ET_{soil} data to non-precipitation days. We also removed days with extremely shallow water tables (<20 cm) when the capillary fringe extends near or to the soil surface, obscuring diel ET-driven soil moisture patterns (Gillham, 1984).

Resulting ET_{soil} measurements and mean ET_{soil}:PET ratios were compared among plots to assess forest structure controls (e.g., LAI or BA), prescribed fire effects, and differences among pine species on plot-scale ET. To evaluate fire effects, we used paired t-tests to compare ET_{soil}:PET at 1-month, 2-months and 3-months post-fire with values observed in the month preceding the fire. To test for species-level differences in ET_{soil}, we compared the fitted slope between ET_{soil}:PET and LAI for slash pine (n = 18), longleaf pine (n = 5) and other pine (loblolly and sand pine, n = 5) stands. Significant differences in slopes were interpreted as species-specific impacts of LAI variation, with larger slopes indicating greater water use per unit LAI. This approach was necessary because the range and distribution of LAI for each species were not consistent (i.e., mean LAI = 1.75, 0.74 and 1.24 for slash, longleaf and other, respectively), precluding direct comparison of water yield by species without LAI normalization.

Finally, gap-filling ET_{soil} data for missing data due to days with precipitation, very shallow water tables, or equipment failure was necessary for water yield quantification at the annual scale (see Section 2.6). To do so, we constructed regression models to predict plot-scale ET_{soil} using daily TSM, PET, 7-day antecedent rainfall, and water-table depth data as explanatory variables. The proportion of ET_{soil} variation explained by these models varied across plots, indicating inherent differences in their hydrogeologic behavior. We selected the regression model for each data gap based on the best-performing (highest R^2) model for which explanatory data were available (e.g., using only PET and antecedent rainfall when TSM or WT data were absent). Importantly, gap-filling in this way double-counts ET losses on rainy days because water is lost both from soil and interception storages. To correct this, we adjusted ET_{soil} on all gap-filled days by subtracting estimated evaporation from interception storage.

2.5. Interception

Because forest interception can be a large fraction of precipitation (Singh & Szeicz, 1979) and differs significantly among stands in response to structural and compositional attributes (LAI,) (Pypker et al., 2005), explicitly accounting for this ET component is critical to water yield estimates. In previous work (Acharya et al., 2020), we developed a novel soil moisture-based approach to estimate forest interception, which we used along with the soil moisture data described above to estimate daily interception for each study plot (Figure 1b). That method estimates total forest (canopy and groundcover) interception storage capacity (B_s) using observed responses of soil moisture (θ) at the 15-cm sensor depth during rainfall events, with individual storms separated by at least 72 hr to ensure both the canopy and groundcover interception storages were dry. Plot-specific relationships between θ and rainfall depth revealed clear rainfall thresholds necessary to induce a soil moisture response, which together with estimated evaporation and soil infiltration during the storm, represents B_s for each plot (Equation 10 in Acharya et al., 2020). Plot-specific B_s values and daily precipitation were then used in a physically-based, continuous interception model developed by Liu (1997, 2001):.

$$I = B_s (D_0 - D) + \int_0^T (1 - D) E \, dt \quad (3)$$

where I is interception, E is evaporation rate from wetted surfaces, and D_0 and D are forest dryness index values at the beginning of a rain event and time T, calculated as:

$$D = 1 - \frac{C}{B_s} \tag{4}$$

where C is the "adherent storage" (water that does not drip to the ground), given by

$$C = B_s \left(1 - D_0 \exp\left(-\frac{(1-\tau)P}{B_s}\right)\right) \tag{5}$$

where τ is the free throughfall coefficient. Interception at each time step, t, is then given by the numerical version of Equation 5, expressed as:

$$I = B_s (D_{t-1} - D_t) + \frac{1}{2}\left[E_{t-1}(1 - D_{t-1}) + E_t (1 - D_t)\right] \tag{6}$$

Finally, the estimates of I given by Equation 6 were summed to obtain daily and annual interception losses from each plot. Further method details are in Acharya et al. (2020). We build on this work by relating annual interception to stand structural attributes (i.e., LAI) and using estimated interception in our calculation of annual water yield.

2.6. Water Yield

We determined annual water yield (Y_w) as the difference between annual precipitation and annual ET (where ET is the sum of ET_{soil} and interception) and evaluated the bi-variate relationship of Y_w with LAI as a first measure of management effects. We further developed a series of multivariate models with predictors including LAI, BA, GC, WT depth, and annual aridity index (PET:P) (Figure 1). We first considered plot identity as a random effect to account for replicated annual measurements. However, since our ultimate goal was a predictive model applicable in new locations based on measurable site and forest attributes, this approach was complemented using a fixed-effects general linear model (GLM) that omitted the plot effects. Site-level random effects were omitted in both models to ensure that effects of attributes such as aridity and groundwater depth could be estimated. We further compared models that used WT depth as a continuous variable (annual mean depth) with those using a binary variable (1 for deep WT sites and 0 for shallow WT sites). Because sites were selected from contrasting hydrogeologic settings (confined vs. unconfined aquifer), resulting groundwater depths were strongly bi-modal (Figure S3 in Supporting Information S1), supporting the use of the binary approach. Crucially, forward application of any resulting model to new sites is substantially simplified using maps of aquifer confinement (i.e., binary depths) rather than relying on spatially distributed estimates of local WT depth (e.g., the USDA SSURGO soil survey), which we found to poorly represent water tables measured at our sites. We selected final models using the minimum Akaike Information criterion (AIC) and evaluated model performance using R^2 and root mean square error (RMSE). For the fixed-effects model assessment, we used a 10-fold cross-validation. All analyses were performed in *R* (v.4.0.2) (Team, 2020) using the *nlme* package for mixed effects model fitting, and the *caret* package for model cross-validation.

3. Results

3.1. Quantifying ET_{soil}

We observed a wide range of soil water loss rates (ET_{soil}) within and across plots and sites (Figure 2), with values consistently lower than PET (though we note that ET_{soil} does not include interception losses). Plot-scale daily ET_{soil} and PET were always positively correlated, but there was marked heterogeneity in fitted slopes among plots, even within the same site (Figure 2 shows data for two sites; similar plots are provided for the other three sites in Figures S7, S8, and S9 in Supporting Information S1). While the ET_{soil}:PET correlation at any given plot was modest (mean $R^2 = 0.33$; $0.03 \leq R^2$ 0.56), the number of days for which ET_{soil} estimates were available provides high confidence in the fitted slopes (range = 0.07–0.65; standard errors between 0.02 and 0.04 in Figure 2). As such, while there is uncertainty about ET_{soil} estimates on any given day, the broad, plot-specific patterns observed are remarkably stable and span a wide range of sensitivity to atmospheric conditions (i.e., the

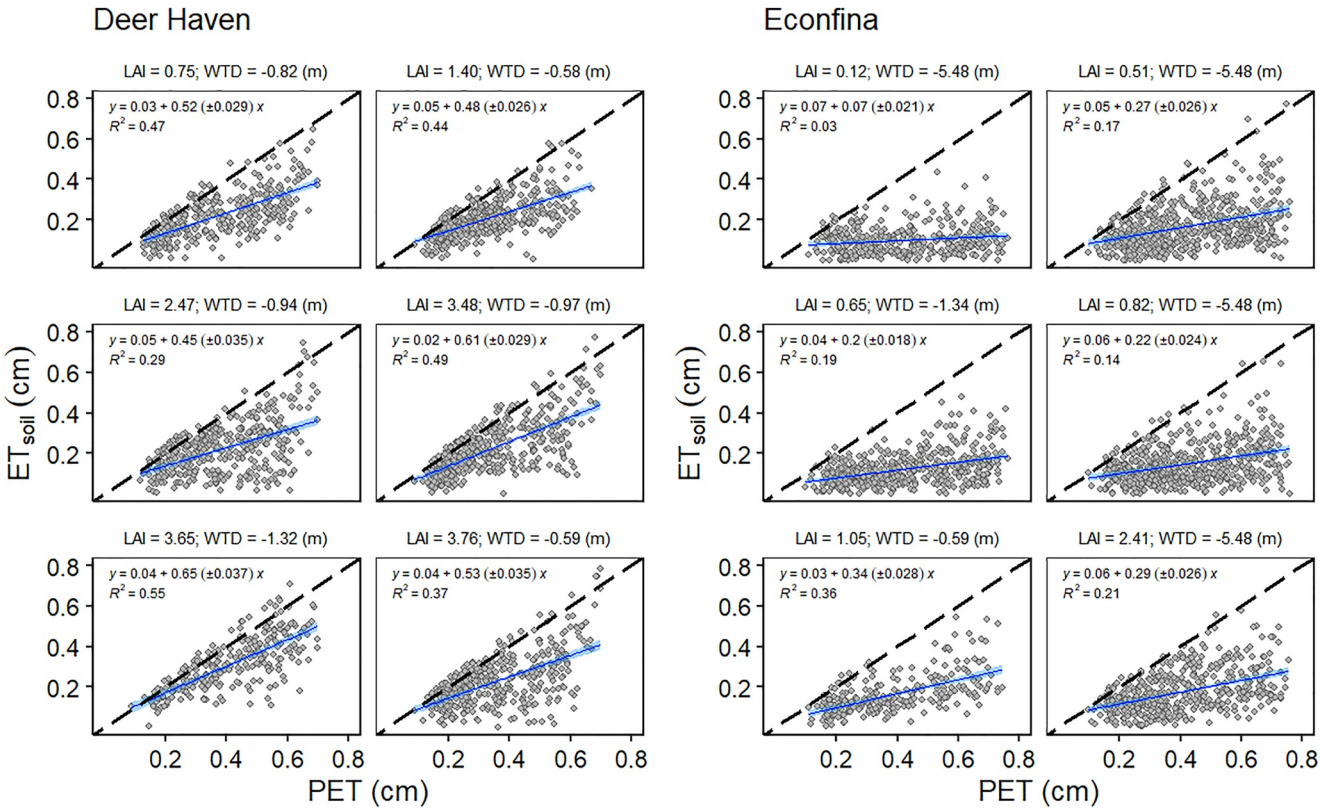

Figure 2. Daily values of soil-moisture derived estimates of ET_{soil} versus potential evapotranspiration (PET) for two of five sites (6 plots each): (a) Deer Haven, where the regional karst aquifer is confined, resulting in a shallow surficial aquifer water table (WT) and (b) Econfina, where the regional aquifer is unconfined resulting in a far deeper WT. Plots within site are organized by leaf area index. The fitted slope (blue line) is shown with standard error estimates (± slope values, blue shading) to illustrate confidence in the ET_{soil}:PET relationship. Similar relationships for the other three sites area available at the associated repository.

range in fitted slopes). As further support of the validity of these ET_{soil} estimates, multiple regression models developed to gap-fill missing ET_{soil} data using PET and metrics of water availability (TSM, WT depth, 7-day antecedent precipitation) substantially outperformed (mean $R^2 = 0.46$; $0.22 \leq R^2$ 0.67) models using PET alone (mean $R^2 = 0.32$, $0.04 \leq R^2$ 0.55), helping to explain residuals in bivariate ET_{soil} versus PET relationships.

3.2. Forest Structure Controls on ET_{soil} and Interception

Forest attributes varied at both site and plot levels (Table 1), providing meaningful gradients to assess structural controls on observed ET_{soil}. Both linear regression slopes (Figure 2) and plot-scale ET_{soil}:PET ratios (Figure 3a) exhibited consistently positive and highly predictive (i.e., slopes have low standard errors) associations with LAI. Specifically, we observed lower slopes in plots with lower LAI (Figure 2), yielding a moderate global ET_{soil}:PET versus LAI relationship across plots ($R^2 = 0.41$; Figure 3a). We focus on LAI as the dominant forest structural controls on ET_{soil} (Figure 3a), noting that despite strong covariance between plot LAI and BA ($r = 0.81$, $p = < 0.001$), using BA yielded a substantially weaker association with ET_{soil}:PET ($R^2 = 0.22$; p-value = 0.008). Annual interception loss ranged from 18.8 to 38.0 cm (Table 1) and, like ET_{soil}, were significantly associated with LAI (Figure 3b).

3.3. Additional Forest Management Controls on ET_{soil}

A potential secondary control on ET_{soil} (and thus water yield) in southeastern pine forests is the use of prescribed fire for understory competition control and habitat improvement. While this study was not designed to investigate fire effects directly, seven plots had low intensity, prescribed fires occur during the study period. At these plots, the change in ET_{soil}:PET between the month prior to the fire versus values one, two, and 3 months post-fire

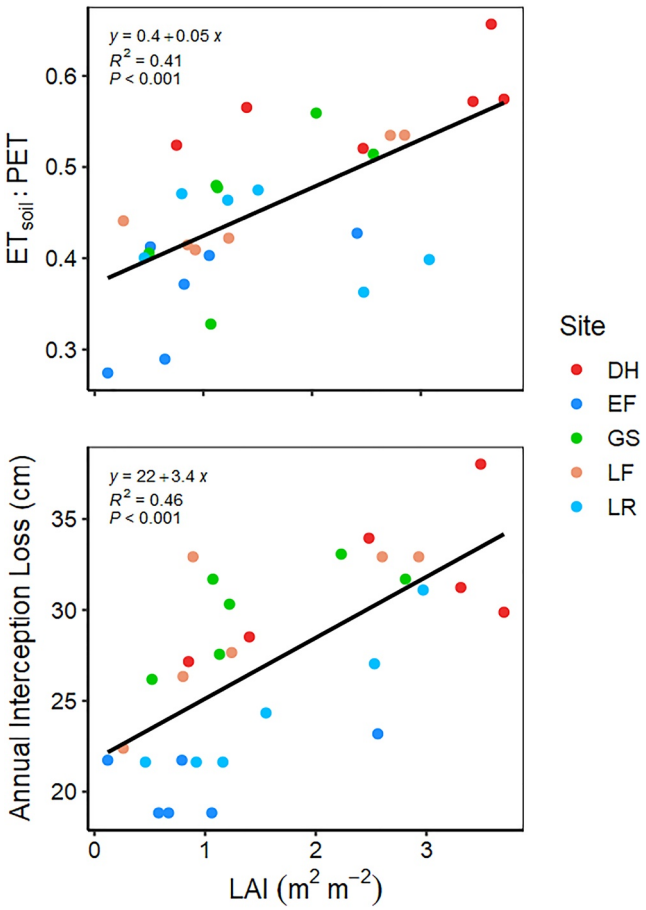

Figure 3. Extracted global associations between leaf area index and (a) ET_{soil}:PET and (b) annual interception loss. Both relationships are highly significant, albeit with clear site effects (plots are color coded by site).

indicate a significant but small and short-lived fire effect (Figure 4a). Specifically, 1-month post-fire ET_{soil}:PET values were significantly ($p < 0.001$) reduced by an average of 8% across the seven sites compared to pre-fire values (range −18% to + 2%; standard deviation, SD = 6%). The effect was short-lived, however, with insignificant differences in ET_{soil}:PET values from pre-fire values in months 2 and three post-fire. As such, while there is a clear prescribed fire effect, the magnitude appears to be small and short-lived compared to natural variation in ET_{soil}:PET.

Dominant pine species also varied across plots, allowing us to assess the influence of species on ET_{soil}. Our comparison of species effects was confined to two species (*P. elliottii* with 16 plots and *P. palustris* with 5 plots), with an additional category of "other pines" (including *P. clausa* with 2 plots and *P. taeda* with 2 plots). Results (Figure 4b) indicate considerable heterogeneity in the fitted slope between ET_{soil}:PET and LAI across plots with the same species, but with no significant differences among species. Linear slopes for slash pine (slope ± std. error = 0.071 ± 0.023) were marginally greater than for longleaf (0.067 ± 0.017) and other pines (0.065 ± 0.031). Overall, these data suggest that water yield variation with LAI is effectively uniform across pine species, at least at the scale of our measurements.

3.4. Water Yield

Estimated Y_w (cm yr^{-1}) for each of the four study years and 30 plots illustrates substantial variation among sites (different colored bars), within sites (individual bars), and over time (comparing bars between years) (Figure 5a). We consistently observed the highest overall Y_w at the EF site in the Florida panhandle and the lowest values at the DH site in the north-central peninsula. Climatic control on Y_w was evident, with significant inter-annual variation within sites, particularly for the plots at the DH site, which in 2014 and 2017 had far higher mean Y_w (44 and 40 cm, respectively) in response to higher rainfall (150 and 136 cm, respectively), than in 2015 and 2016 (Y_w of 19 and -7 cm, respectively) when annual rainfall of was lower (127 and 107 cm); the results for 2016, in particular, indicate net utilization of shallow groundwater.

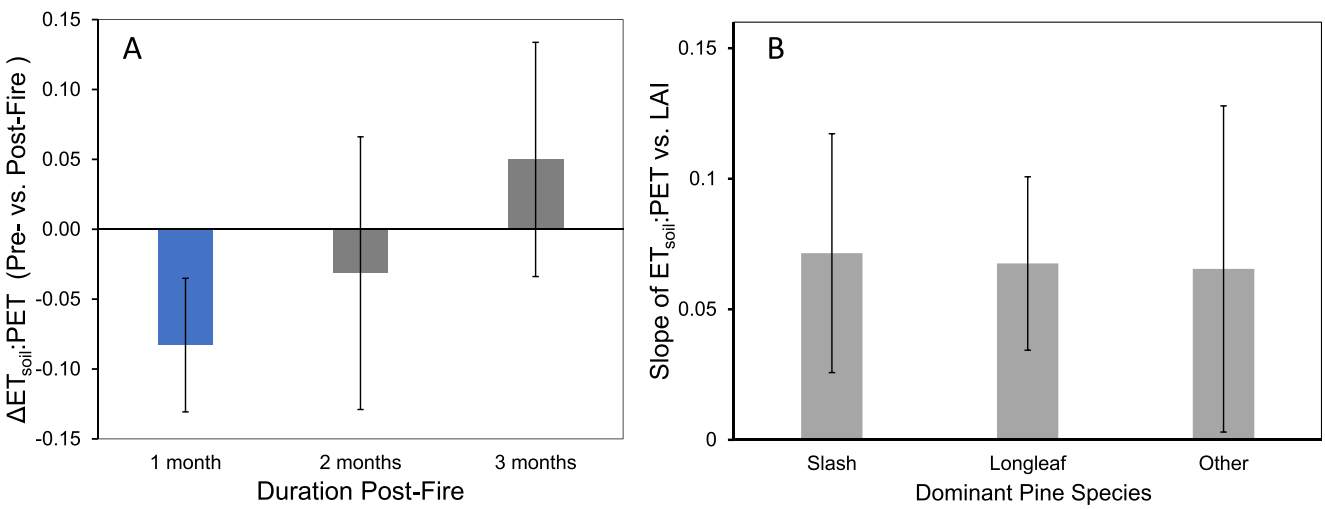

Figure 4. Summary of measured effects of (a) prescribed fire and (b) dominant pine species on variation in ET_{soil}:PET; error bars in both panels are 95% confidence intervals. We observed a significant decline (mean = 0.08, $p < 0.001$) in the month following prescribed fire ($n = 7$ sites), but no detectable longer-term effect. There was no significant difference in the fitted slope of ET_{soil}:PET versus leaf area index for any of the dominant pine species in the study.

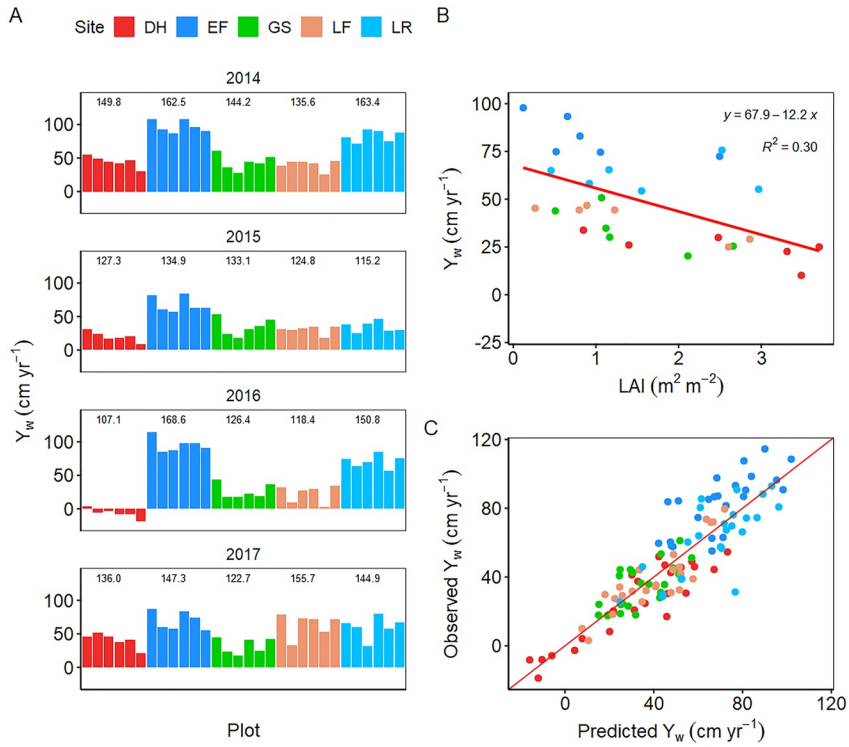

Figure 5. (a) Plot-wise water yield (Y_w) estimates (cm yr^{-1}) by year for the five sites during 2014–2017. The numbers above the bars are the annual rainfall amounts at each site. (b) Relationship between plot-scale Y_w and leaf area index. (c) Scatter plot of observed Y_w and model predictions ($R^2 = 0.78$, $p < 0.001$) from the general linear model (Table 3).

Plot-level variation in Y_w was substantial and strongly linked to forest structure, with increased LAI predicting higher ET_{soil} and higher annual interception (Figure 3), resulting in lower Y_w (Figure 5b). Concordantly, all candidate multivariate models used LAI as the most predictive forest structural attribute (as opposed to BA and understory cover). Table 2 summarizes the regression slopes for the LAI term in models with plot-level random effects and groundwater depth as a binary value (i.e., deep vs. shallow), indicating a 9.7 cm yr^{-1} decrease in Y_w for each unit increase in LAI in the lowest AIC model. This model explained 93% of the extant variation in annual Y_w across plots with a RMSE of 7.9 cm yr^{-1}. In addition to LAI, this model also included main effects of aridity and groundwater depth, suggesting that Y_w increases by approximately 17 cm yr^{-1} under deep WT conditions and decreases with increasing aridity, with a 17.8 cm yr^{-1} reduction for a 1-standard deviation increase in aridity ($\sigma_{aridity} = 0.13$). Models using continuous WT depth rather than binary depth had reduced performance (AIC values of 1000.5 vs. 995.1 for continuous and binary groundwater models, respectively). This result, and the fact that binary groundwater depths are more readily available and applicable to new sites, supports use of binary groundwater depths for discussion of all subsequent results.

Model performance using the same structure (i.e., $Y_w \sim$ LAI + GW + Arid) but without plot-level random effects (Table 3) resulted in negligible changes in regression parameters for all three variables, but reduced model goodness of fit ($R^2 = 0.78$; Figure 5c) and increased RMSE to 14.3 cm. Notably, however, 10-fold cross-validation yielded model performance that was scarcely reduced (mean $R^2 = 0.76$, mean RMSE = 14.9), suggesting the model is stable and not overfitted, supporting Y_w predictions at unmeasured locations.

Table 2
Summary of Mixed Model (Including Plot-Level Random Effects) Performance With Predictors Including: Leaf Area Index, Aridity Index (Arid), Binary Groundwater Depth (1 – Deep, 0 – Shallow), Ground cover, Basal Area, and Dominant Pine Species

Model structure	AIC	Fitted LAI slope (cm yr^{-1})	Model R^2
$Y_w \sim$ LAI	1086.5	−12.1	0.65
$Y_w \sim$ LAI + Arid	915.5	−11.0	0.92
$Y_w \sim$ LAI + GW	1064.3	−10.0	0.63
$Y_w \sim$ LAI + Arid + GW	**900.6**	**−9.7**	**0.93**
$Y_w \sim$ LAI + Arid * GW	901.7	−9.7	0.94
$Y_w \sim$ LAI + Arid + GW + GC	904.4	−10.6	0.93
$Y_w \sim$ LAI + Arid + GW + BA	904.2	−10.3	0.93
$Y_w \sim$ LAI + Arid + GW + SPP	903.3	−9.4	0.93

Note. Fitted LAI slopes are also provided. The selected model (bold) was chosen based on the lowest AIC, and interpretive simplicity.

Table 3
General Linear Model of Water Yield (Y_w in cm yr^{-1}) as a Function of Aridity Index (PET:P), Leaf Area Index, and Groundwater Depth (1 – Deep, 0 – Shallow) Without Plot-Level Random Effects

Variables	Estimate	Std. Error	t-value	Pr(>|t|)
Intercept	197.6	10.8	18.3	<0.0001
PET:P	−137.2	10.1	−13.6	<0.0001
LAI	−9.7	1.2	−8.1	<0.0001
GW	16.8	2.8	6.0	<0.0001

Note. Model null deviance is 94456 (df = 119), with residual deviance of 20809 (df = 116), indicating 78% of null deviance is explained.

4. Discussion

Across ecosystems types, robustly quantifying ET is critical for understanding water balance components and guiding coupled water and natural resources management (Apsalyamova et al., 2015). In forests, this is challenging but central to improving our ability to predict changes in stand-scale water yield resulting from forest management activities and informing tradeoffs among forest product production and hydrologic services (Schwaiger et al., 2019). In this work, we overcome the limitations of current approaches for estimating ET and resulting water yield (coarse resolution, high expense) by collecting temporally and spatially dense *in-situ* data to produce simple, operationalizable models that appear to effectively predict water yield as a function of forest structure, hydrogeological setting, and climate (Figure 1).

4.1. In-Situ ET_{soil} Measurements

In this work, we quantified ET losses across 30 forest stands by applying a soil moisture-based method (Nachabe et al., 2005) for daily ET_{soil} along with complementary interception measurements (Acharya et al., 2020). Compared to other methods, which can be prohibitively expensive (e.g., eddy covariance) or integrate over far larger scales (e.g., catchment water budgets), this approach quantifies ET variation at stand scales, enabling investigation across geographic, edaphic, and forest management gradients. While the inferential advantages of soil moisture-based ET_{soil} measurements are clear, a few methodological considerations merit discussion. First, soil moisture measurements are point-scale and thus require dense sensor instrumentation to capture variation with depth and across different stand locations. To capture this variation, we installed three soil profiles per plot, each with 5–6 sensors, yielding a total of 564 soil moisture sensors across the study, with attendant installation, acquisition, and data management challenges. We note that our study sites are dominated by fine sands, with rapid vertical and lateral soil moisture redistribution therefore expected. However, the degree to which we captured finer-scale variation in soil moisture dynamics (and thus correctly imputed plot-level ET_{soil}) remains unknown. This uncertainty and the associated need for even denser instrumentation in less conductive soils may complicate method application in other settings. Second, data gaps were common due to precipitation events, sensor failures, and WT depths that precluded soil moisture integration with our sensor discretization (e.g., <20 cm). However, strong relationships between $ET_{soil,}$ climate (PET), and co-measured predictors of water availability supported successful gap-filling, which allowed for consistent, daily water yield quantification for summation to annual values. Finally, the method assumes that sensor measurements entirely bound the region from which water for ET is sourced; as such, the moisture conditions and temporal dynamics at the bottom sensor are of particular importance. In the supplemental information (Figures S4, S5, and S6 in Supporting Information S1), we show that this assumption was largely met in this study, with far higher and more stable soil moisture at the lowest sensor, even in settings where the WT was more than 5 m below ground. Further, while tap root depths in southeastern coastal plain systems can exceed 3m (Samuelson et al., 2017), the vast majority (ca. > 90%) of root biomass typically occurs within 1 m in our study systems (Domec et al., 2012; Van Rees & Comerford, 1986) and within 2 m in other global biomes (Schenk & Jackson, 2002).

Having met these methodological considerations, our high-frequency soil moisture measurements yielded ET_{soil} estimates that varied as expected across forest structure gradients (e.g., LAI) and generally aligned with climate drivers (i.e., PET and water availability). Under well-watered and standardized vegetation conditions, we would expect 1:1 correspondence between actual ET and PET (Irmak & Haman, 2003; Shoemaker & Sumner, 2006). Across a range of vegetation and moisture conditions, ET should at least be strongly positively correlated with PET, with departure from 1:1 correspondence driven by a combination of water availability (Jung et al., 2010; Wetzel & Chang, 1987) and plant structural properties (Baldocchi et al., 2004; Li et al., 2016). This aligns with our expectations that at all experimental plots, relationships between ET_{soil} and PET were positive and statistically significant ($p < 0.05$, Figure 2). All fitted slopes were <1 (i.e., $ET_{soil} < PET$), with nearly all daily data falling below the 1:1 line, but we note that ET_{soil} does not include canopy interception (and subsequent evaporation) and thus does not represent total ET. Multiple regression models including both PET and water availability metrics were better predictors of ET_{soil}, highlighting the short (PET) and medium (total soil moisture) time scales over which climate controls ET_{soil} and further supporting the viability of ET_{soil} estimates from soil moisture dynamics.

As expected, we found that forest structure strongly influenced the relationship between ET_{soil} and PET. While consistently positive associations suggest our ET_{soil} estimates broadly reflect climatic conditions, PET alone explained only between 3% and 55% of estimated ET_{soil} variance and was worst in low LAI plots (e.g., 1 through 4 at EF, all with LAI < 1.0; Figure 2). In addition to the low R^2 values, those sites also exhibited shallow slopes, suggesting ET_{soil} is relatively invariant to changing PET values in low biomass plots. In contrast, for plots with LAI > 1.0, the relationship between ET_{soil} and PET was stronger (mean $R^2 = 0.36$.) and better aligned with literature values from forested watersheds in the southeastern US. For example, Lu et al. (2005) observed PET versus ET correlations (from a watershed mass balance) between 0.57 and 0.65 (i.e., R^2 from 0.32 to 0.42) depending on the PET model used. Broad alignment of ET and PET associations across disparate studies and methods underscores the utility of the Nachabe et al. (2005) method, particularly where variability at intermediate spatial scales is of interest.

4.2. Leaf Area Index Predicts ET_{soil}, Interception, and Water Yield

Leaf area index (LAI) was the most important forest attribute for predicting stand-scale water balances, explaining 41%, 46%, and 30% of the variance in ET_{soil}:PET, interception, and water yield, respectively (Figures 3 and 5b). While other forest attributes covaried with LAI (e.g., $r = +0.81$ with BA, $r = -0.53$ for groundcover), LAI was consistently the strongest predictor of the stand water balance. Further, we observed consistent ET_{soil}:PET versus LAI associations across all pine species, suggesting that species replacement (e.g., loblolly to longleaf restoration) without attendant LAI reductions are unlikely to result in significant water yield improvements. Our results align with many studies identifying LAI as the best predictor (along with climate (Edwards & Troendle, 2012)) of forest water use and yield. For example, McLaughlin et al. (2013) found LAI explained 53% of the variance in ET:annual precipitation in southeastern US pine forests, Del Grosso et al. (2018) found remotely sensed Normalized Difference Vegetation Index (which strongly covaries with LAI (Q. Wang et al., 2005)) explained 50%–52% of observed variability in daily ET in shortgrass steppe, and Sun, Alstad et al. (2011) found LAI to be the strongest predictor of monthly ET across a diversity of ecosystems in the US, China, and Australia. As such, our stand-scale, empirical results align with expectations of the structural drivers of water yield and further support the long-standing contention (e.g., Bosch & Hewlett, 1982) that forest structure management (via LAI changes) can impact water yield at local scales.

The importance of LAI in controlling ET_{soil} and interception (and, by extension, water yield) follows from the role of leaf surfaces as the primary exchange site between forests and the atmosphere (Vose et al., 1994) and as temporary storage for incoming precipitation (Savenije, 2004). While LAI emerges as the keystone forest attribute for understanding stand water use, foresters rarely measure it, often relying on BA, density, and stand age to characterize structure (Van Laar & Akça, 2007). This gap highlights the utility of allometric relationships between BA and LAI for specific forest types (C. Gonzalez-Benecke et al., 2014), as well as satellite or LIDAR remote sensing to accurately reproduce field-measured LAI (Blinn et al., 2019; Kinane et al., 2021). For example, the Moderate Resolution Imaging Spectroradiometer provides global LAI estimates every 1–2 days at 500 m spatial resolution, and Landsat produces LAI every 16 days at 30-m resolution (Blinn et al., 2019). At smaller scales, LIDAR-derived estimates of LAI are reliable and can be used to monitor within- and between-stand variation (Almeida et al., 2019), which are critical for robust predictions of landscape water yield. Large-scale, dynamic surveillance of this key attribute is integral to quantitatively monitoring changes in ET and water yield over time. Given the strong mechanistic connection and empirical relationship between LAI and water yield, remotely sensed LAI is likely to serve as the key tool for low-cost validation of payment-for-ecosystem service programs that compensate forest landowners for "enhancing" water yield in lieu of maximum timber production.

4.3. Temporal and Spatial Variance in Water Yield

Our field measurements and models offer insight into temporal and spatial variation in pine forest water yield. We observed substantial inter-annual variation in water yield in response to climatic variability. Plot-specific water yields varied by as much as 60 cm over the 4-year study (mean range = 38 cm, mean temporal CV = 0.48), primarily in response to annual rainfall variation (mean temporal CV = 0.11), since plot level PET was effectively constant (mean temporal CV = 0.04). For example, at the DH site, where water yield was consistently low, five of the six plot values were negative in the driest year (2016; Figure 5a). Forest structure and thus LAI controls on water yield can also be temporally dynamic particularly in plantation rotations (C. A. Gonzalez-Benecke

et al., 2012), although LAI was relatively stable during our 4-year study (mean plot CV = 0.15). In addition to stand development, fires that alter canopy structure can also influence the temporal trajectory of LAI, and thus water yield. In this work, we only assessed effects of prescribed fire aimed at reducing understory biomass and tree regeneration (and thus maintaining low LAI) in stands for which fire frequency was already high (e.g., every 2–5 years). The modest and short-duration declines in post-fire ET_{soil}:PET (Figure 3) suggest minor LAI losses and rapid recovery. While temporal variability in LAI was thus minimal during our study period, clear associations between water yield and LAI indicate the potential water yield changes with time following management actions that increase (e.g., via rotation age, decreased fire frequency) or reduce (e.g., via thinning, increased fire frequency) forest biomass.

Spatial variation in the landscape controls on water yield are crucial elements of regional and larger-scale predictions. For example, despite the geographic proximity of our sites, aridity variation was relevant, with site means varying between 0.94 and 1.09. Indeed, spatial variation in aridity between sites (CV = 0.11) was of comparable magnitude to the temporal variation within sites (CV = 0.13), underscoring the importance of both sources of variability for water yield predictions. A further source of spatial variation across our sites was hydrogeologic setting, which operationally represents groundwater depth. This factor, treated as a binary variable (i.e., "deep" where the Floridan aquifer is unconfined, and "shallow" where a surficial aquifer is perched on a confining unit) exerted strong influence on the magnitude of water yield, with model estimates indicating 17 cm greater water yield in unconfined settings. This aligns with known patterns of recharge across the state (Phelps, 1984) and illustrates the important role that shallow WT conditions play in supplying phreatic water to support primary production in Florida's sandy soils (Sun et al., 1998). Notably, the combined regional variation in aridity and WT depth was larger than the effects of LAI on water yield; the standardized slope (i.e., fitted slope divided by the variable's standard deviation) is 18 cm for aridity, but only 10 for LAI. This implies that intrinsic site attributes are the dominant control on the magnitude of water yield. However, because LAI can be managed (and because interaction effects among LAI and other variables did not improve model fit), forest structure modification is a crucial—and independent—water yield control.

4.4. Predicting and Managing Forest Water Yield

Strong empirical associations between water yield and a small number of site-level variables allow us to make robust predictions across the varying hydrogeologic, edaphic, and forest structural attributes of our study sites, and over time with dynamic climate conditions. While including plot-level random effects improves model performance ($R^2 = 0.93$, AIC = 900.6) over the more general model ($R^2 = 0.78$, AIC = 969.2), it does so at the expense of model generality and use for forward-looking management applications. Specifically, coupling widely available climate and hydrogeology data with field measured or remotely sensed LAI data can enable short- and long-term predictions of water yield across our study region. Forward model applications include scenario analyses to predict changes in water yield with different forest management activities, short-term climate variation, and long-term climate change at spatial scales from forest stands to large watersheds. In the southeastern US and other regions facing increasing water shortages (Anandhi & Bentley, 2018; Sun, 2013), such region-specific models are critical for supporting water supply planning activities (Douglass, 1983) and the development and implementation of policy instruments that incentivize water yield as an important forest product (Bawa & Dwivedi, 2021; Susaeta et al., 2016, 2017). While coarser watershed and continental-scale models exist (e.g., the Water Supply Stress Index Model, WaSSI (Sun, Caldwell, et al., 2011)) and similarly offer estimates of water yield change with land use and climate scenarios, empirical predictions from *in-situ* observations are important for supporting and validating more region- and ecosystem-specific models. Still, our modeled stand-level water yield responses to lower LAI may be higher than cumulative watershed effects due to potential damping of water yield signals at larger scales via increased internal storage or enhanced ET in other watershed locations. Further work to connect stand-level measurements to watershed-scale responses, including internal storage dynamics, may be necessary to ultimately validate the predictions made here and ensure that forest management incentives created for water supply planning are based on achievable and verifiable water yield gains.

Forest management contributions to sustainable water supply planning are complicated by population growth (Zwick & Carr, 2006), agricultural intensification (S. J. Lawrence, 2016), and increasing global demand for wood and forest bioenergy products (Galik & Abt, 2016; McNichol et al., 2019). Projected climate change will exacerbate these stressors and further threaten regional water sustainability. Precipitation projections for the southeast

are uncertain (Kunkel et al., 2013), but include more extremes (droughts, large storms) and an overall decrease in annual rainfall, particularly during summer (Konrad & Fuhrmann, 2013). Meanwhile, mean annual temperatures are projected to rise, increasing ET and decreasing "available precipitation" (Sun, McNulty, et al., 2008). Recent estimates indicate ET increases of ca. 10% from 2003 to 2019, with concordant decreases in water yield (Pascolini-Campbell et al., 2021), further highlighting increasingly difficult tradeoffs among food, energy, and water resources (W. Wang et al., 2015).

The relatively simple model developed here is useful for evaluating wood-water tradeoffs in the context of other competing water uses and economic considerations. Managing tradeoffs is increasingly part of the water supply planning arena (Hallema et al., 2019; Melo et al., 2021; Willaarts, 2012). Critically, programs that incentivize forest management for increased water yield (Douglass, 1983) may simultaneously meet other environmental objectives that require lowered forest density (e.g., endangered species habitat, diversity enhancements). Crucial to these efforts are operational models of water yield that provide robust scenario predictions, but also fair and equitable water yield pricing structures and careful program development to ensure a viable forest industry in the southeastern US and more broadly. The empirical models developed here are an important step in this integrated landscape planning, and the methods used to arrive at these models may be applicable to other regions.

Data Availability Statement

Raw data, ET_{soil} graphs for all sites, maps and photographs of the selected sites, and plots of ancillary time series can be found at http://www.hydroshare.org/resource/a55dfb0494864847b735e3c65ee0caf8.

Acknowledgments
We gratefully acknowledge field technicians Kenyon Watkins, Paul Decker, Brett Caudill, Kevin Henson, and Kenny Duffield. Funding was provided by all five Water Management Districts in Florida, as well as the Florida Department of Agriculture and Consumer Services (FDACS) under contract number 20834. We gratefully acknowledge project oversight and field site coordination from Bill Bartnick (FDACS), Stephen Miller (SJRWMD), Bob Heeke (SRWMD), Sean King (SWFWMD), Jeff Sumner (SFWMD) and Bill Cleckley (NWFWMD), as well as project visioning from Dr. Ann Shortelle (SJRWMD) and Jeff Vowell (FFS).

References

Acharya, S., McLaughlin, D., Kaplan, D., & Cohen, M. J. (2020). A proposed method for estimating interception from near-surface soil moisture response. *Hydrology and Earth System Sciences*, *24*(4), 1859–1870. https://doi.org/10.5194/hess-24-1859-2020

Almeida, D. R. A. D., Stark, S. C., Shao, G., Schietti, J., Nelson, B. W., Silva, C. A., et al. (2019). Optimizing the remote detection of tropical rainforest structure with airborne lidar: Leaf area profile sensitivity to pulse density and spatial sampling. *Remote Sensing*, *11*(1), 92.

Anandhi, A., & Bentley, C. (2018). Predicted 21st century climate variability in southeastern US using downscaled CMIP5 and meta-analysis. *Catena*, *170*, 409–420. https://doi.org/10.1016/j.catena.2018.06.005

Apsalyamova, S. O., Khuazhev, O., Khashir, B., Tkhagapso, M. B., & Bgane, Y. K. (2015). The economic value of forest ecosystem services. *Journal of Environmental Management and Tourism*, *6*(2), 291.

Baldocchi, D. D., Xu, L., & Kiang, N. (2004). How plant functional-type, weather, seasonal drought, and soil physical properties alter water and energy fluxes of an oak–grass savanna and an annual grassland. *Agricultural and Forest Meteorology*, *123*(1–2), 13–39. https://doi.org/10.1016/j.agrformet.2003.11.006

Bawa, R., & Dwivedi, P. (2021). Estimating marginal costs of additional water flow from a loblolly pine stand in south Georgia, United States. *Journal of Forestry*, *119*(4), 329–336. https://doi.org/10.1093/jofore/fvab010

Becknell, J. M., Desai, A. R., Dietze, M. C., Schultz, C. A., Starr, G., Duffy, P. A., et al. (2015). Assessing interactions among changing climate, management, and disturbance in forests. *A Macrosystems Approach*, *65*(3), 263–274. https://doi.org/10.1093/biosci/biu234

Bell, J., & Lovelock, C. E. (2013). Insuring Mangrove forests for their role in mitigating coastal erosion and storm-surge: An Australian case study. *Wetlands*, *33*(2), 279–289. https://doi.org/10.1007/s13157-013-0382-4

Blinn, C. E., House, M. N., Wynne, R. H., Thomas, V. A., Fox, T. R., & Sumnall, M. (2019). Landsat 8 based leaf area index estimation in loblolly pine plantations. *Forests*, *10*(3), 222. https://doi.org/10.3390/f10030222

Bonan, G. B. (2008). Forests and climate change: Forcings, feedbacks, and the climate benefits of forests. *Science*, *320*(5882), 1444–1449. https://doi.org/10.1126/science.1155121

Bosch, J. M., & Hewlett, J. (1982). A review of catchment experiments to determine the effect of vegetation changes on water yield and evapotranspiration. *Journal of hydrology*, *55*(1–4), 3–23. https://doi.org/10.1016/0022-1694(82)90117-2

Brown, A. E., Zhang, L., McMahon, T. A., Western, A. W., & Vertessy, R. A. (2005). A review of paired catchment studies for determining changes in water yield resulting from alterations in vegetation. *Journal of hydrology*, *310*(1–4), 28–61. https://doi.org/10.1016/j.jhydrol.2004.12.010

Cecílio, R. A., Pimentel, S. M., & Zanetti, S. S. (2019). Modeling the influence of forest cover on streamflows by different approaches. *Catena*, *178*, 49–58. https://doi.org/10.1016/j.catena.2019.03.006

Creed, I. F., Jones, J. A., Archer, E., Claassen, M., Ellison, D., McNulty, S. G., et al. (2019). Managing forests for both downstream and downwind water. *Frontiers in Forests and Global Change*, *2*, 64. https://doi.org/10.3389/ffgc.2019.00064

Davie, T., & Fahey, B. (2018). Forestry and water yield: The New Zealand example. *Journal of Forestry*, *49*(4), 3–8.

Del Grosso, S. J., Parton, W., Derner, J. D., Chen, M., & Tucker, C. J. (2018). Simple models to predict grassland ecosystem C exchange and actual evapotranspiration using NDVI and environmental variables. *Agricultural and Forest Meteorology*, *249*, 1–10. https://doi.org/10.1016/j.agrformet.2017.11.007

Domec, J., Sun, G., Noormets, A., Gavazzi, M. J., Treasure, E. A., Cohen, E., et al. (2012). A comparison of three methods to estimate evapotranspiration in two contrasting loblolly pine plantations: Age-related changes in water use and drought sensitivity of evapotranspiration components. *Forest Science*, *58*(5), 497–512. https://doi.org/10.5849/forsci.11-051

Douglass, J. E. (1983). The potential for water yield augmentation from forest management in the Eastern United States 1. *JAWRA Journal of the American Water Resources Association*, *19*(3), 351–358. https://doi.org/10.1111/j.1752-1688.1983.tb04592.x

Downing, J. (2015). Forest thinning may increase water yield from the Sierra Nevada. *California Agriculture*, *69*(1), 10–11. https://doi.org/10.3733/ca.v069n01p10

Dudley, N., Jeanrenaud, J.-P., & Sullivan, F. (2014). *Bad harvest: The timber trade and the degradation of global forests*. Routledge.

Duncker, P. S., Raulund-Rasmussen, K., Gundersen, P., Katzensteiner, K., De Jong, J., Ravn, H. P., et al. (2012). How forest management affects ecosystem services, including timber production and economic return: Synergies and trade-offs. *Ecology and Society*, *17*(4). https://doi.org/10.5751/es-05066-170450

Edwards, P. J., & Troendle, C. A. (2012). Water yield and hydrology. In R. LaFayette, M. T. Brooks, J. P. Potyondy, L. Audin, S. L. Krieger, & C. C. Trettin (Eds.), (Vol. 229–281, pp. 229–281). *2012 Cumulative watershed effects of fuel management in the Eastern United States. Gen. Tech. Rep. SRS-161*. US Department of Agriculture Forest Service, Southern Research Station.

Farley, K. A., Jobbágy, E. G., & Jackson, R. B. (2005). Effects of afforestation on water yield: A global synthesis with implications for policy. *Global Change Biology*, *11*(10), 1565–1576. https://doi.org/10.1111/j.1365-2486.2005.01011.x

Filoso, S., Bezerra, M. O., Weiss, K. C., & Palmer, M. A. (2017). Impacts of forest restoration on water yield: A systematic review. *PLoS One*, *12*(8), e0183210. https://doi.org/10.1371/journal.pone.0183210

Fisher, J. B., Malhi, Y., Bonal, D., Da Rocha, H. R., De Araasjo, A. C., Gamo, M., et al. (2009). The landâ "atmosphere water flux in the tropics. *Global Change Biology*, *15*(11), 2694–2714. https://doi.org/10.1111/j.1365-2486.2008.01813.x

Freeman, J., Kobziar, L., Rose, E. W., & Cropper, W. (2017). A critique of the historical-fire-regime concept in conservation. *Conservation Biology*, *31*(5), 976–985. https://doi.org/10.1111/cobi.12942

Galik, C. S., & Abt, R. C. (2016). Sustainability guidelines and forest market response: An assessment of European Union pellet demand in the southeastern United States. *Gcb Bioenergy*, *8*(3), 658–669. https://doi.org/10.1111/gcbb.12273

García-Nieto, A. P., García-Llorente, M., Iniesta-Arandia, I., & Martín-López, B. (2013). Mapping forest ecosystem services: From providing units to beneficiaries. *Ecosystem Services*, *4*, 126–138. https://doi.org/10.1016/j.ecoser.2013.03.003

Gillham, R. (1984). The capillary fringe and its effect on water-table response. *Journal of Hydrology*, *67*(1–4), 307–324. https://doi.org/10.1016/0022-1694(84)90248-8

Gonzalez-Benecke, C., Gezan, S. A., Samuelson, L. J., Cropper, W. P., Leduc, D. J., & Martin, T. A. (2014). Estimating Pinus palustris tree diameter and stem volume from tree height, crown area and stand-level parameters. *Journal of Forestry Research*, *25*(1), 43–52. https://doi.org/10.1007/s11676-014-0427-4

Gonzalez-Benecke, C. A., Jokela, E. J., & Martin, T. A. (2012). Modeling the effects of stand development, site quality, and silviculture on leaf area index, litterfall, and forest floor accumulations in loblolly and slash pine plantations. *Forest Science*, *58*(5), 457–471. https://doi.org/10.5849/forsci.11-072

González-Sanchis, M., Ruiz-Pérez, G., Del Campo, A. D., Garcia-Prats, A., Francés, F., & Lull, C. (2019). Managing low productive forests at catchment scale: Considering water, biomass and fire risk to achieve economic feasibility. *Journal of Environmental Management*, *231*, 653–665. https://doi.org/10.1016/j.jenvman.2018.10.078

Good, S. P., Noone, D., & Bowen, G. (2015). Hydrologic connectivity constrains partitioning of global terrestrial water fluxes. *Science*, *349*(6244), 175–177. https://doi.org/10.1126/science.aaa5931

Greenwood, A. J., Cresswell, D., Fee, B., & Vanlaarhoven, J. (2008). Sustainable water resources management, plantation forestry and a method for the provision of environmental flows to wetland ecosystems. *Proceedings of Water Down Under 2008*, 2191.

Gribovszki, Z., Kalicz, P., Szilágyi, J., & Kucsara, M. (2008). Riparian zone evapotranspiration estimation from diurnal groundwater level fluctuations. *Journal of Hydrology*, *349*(1–2), 6–17. https://doi.org/10.1016/j.jhydrol.2007.10.049

Hallema, D., Kinoshita, A., Martin, D., Robinne, F., Galleguillos, M., McNulty, S., et al. (2019). Fire, forests and city water supplies. *Unasylva*, *251*(1), 58–66.

Hawthorne, S. N., Lane, P. N., Bren, L. J., & Sims, N. C. (2013). The long term effects of thinning treatments on vegetation structure and water yield. *Forest Ecology and Management*, *310*, 983–993. https://doi.org/10.1016/j.foreco.2013.09.046

Hornbeck, J., Martin, C., & Eagar, C. (1997). Summary of water yield experiments at Hubbard Brook experimental forest, New Hampshire. *Canadian Journal of Forest Research*, *27*(12), 2043–2052. https://doi.org/10.1139/x97-173

Hunter, M. L., Jr. (1990). *Wildlife, forests, and forestry Principles of managing forests for biological diversity*. Prentice Hall.

Irmak, S., & Haman, D. Z. (2003). Evapotranspiration: Potential or reference? *Environmental Data and Information Service*, *2003*(14). https://doi.org/10.32473/edis-ae256-2003

Jayachandran, S., De Laat, J., Lambin, E. F., Stanton, C. Y., Audy, R., & Thomas, N. E. (2017). Cash for carbon: A randomized trial of payments for ecosystem services to reduce deforestation. *Science*, *357*(6348), 267–273. https://doi.org/10.1126/science.aan0568

Jones, C. N., McLaughlin, D. L., Henson, K., Haas, C. A., & Kaplan, D. A. (2018). From salamanders to greenhouse gases: Does upland management affect wetland functions? *Frontiers in Ecology and the Environment*, *16*(1), 14–19. https://doi.org/10.1002/fee.1744

Jones, J. A., Wei, X., Archer, E., Bishop, K., Blanco, J. A., Ellison, D., et al. (2020). Forest-water interactions under global change. In *Forest-water interactions* (pp. 589–624). Springer.

Jung, M., Reichstein, M., Ciais, P., Seneviratne, S. I., Sheffield, J., Goulden, M. L., et al. (2010). Recent decline in the global land evapotranspiration trend due to limited moisture supply. *Nature*, *467*(7318), 951–954. https://doi.org/10.1038/nature09396

Keenan, R. J., Reams, G. A., Achard, F., De Freitas, J. V., Grainger, A., & Lindquist, E. (2015). Dynamics of global forest area: Results from the FAO Global Forest Resources Assessment 2015. *Forest Ecology and Management*, *352*, 9–20. https://doi.org/10.1016/j.foreco.2015.06.014

Kinane, S. M., Montes, C. R., Albaugh, T. J., & Mishra, D. R. (2021). A model to estimate leaf area index in loblolly pine plantations using Landsat 5 and 7 images. *Remote Sensing*, *13*(6), 1140. https://doi.org/10.3390/rs13061140

Komatsu, H., & Kume, T. (2020). Modeling of evapotranspiration changes with forest management practices: A genealogical review. *Journal of Hydrology*, *585*, 124835. https://doi.org/10.1016/j.jhydrol.2020.124835

Konrad, C. E., & Fuhrmann, C. M. (2013). Climate of the southeast USA: Past, present, and future. In *Climate of the southeast United States* (pp. 8–42). Springer.

Kreye, M. M., Adams, D. C., & Escobedo, F. J. (2014). The value of forest conservation for water quality protection. *Forests*, *5*(5), 862–884. https://doi.org/10.3390/f5050862

Kunkel, K. E., Stevens, L. E., Stevens, S. E., Sun, L., Janssen, E., Wuebbles, D., et al. (2013). *Regional climate trends and scenarios for the US national climate assessment Part 4*. Climate of the US Great Plains.

Lawrence, D. M., Thornton, P. E., Oleson, K. W., & Bonan, G. B. (2007). The partitioning of evapotranspiration into transpiration, soil evaporation, and canopy evaporation in a GCM: Impacts on land-atmosphere interaction. *Journal of Hydrometeorology*, *8*(4), 862–880. https://doi.org/10.1175/jhm596.1

Lawrence, S. J. (2016). *Water use in the apalachicola-chattahoochee-flint river basin, Alabama, Florida, and Georgia, 2010, and water-use trends, 1985-2010* Rep. 2328-0328. US Geological Survey.

Lesch, W., & Scott, D. F. (1997). The response in water yield to the thinning of Pinus radiata, Pinus patula and Eucalyptus grandis plantations. *Forest Ecology and Management*, *99*(3), 295–307. https://doi.org/10.1016/s0378-1127(97)00045-5

Li, S., Kang, S., Zhang, L., Zhang, J., Du, T., Tong, L., & Ding, R. (2016). Evaluation of six potential evapotranspiration models for estimating crop potential and actual evapotranspiration in arid regions. *Journal of Hydrology*, *543*, 450–461. https://doi.org/10.1016/j.jhydrol.2016.10.022

Liu, S. (1997). A new model for the prediction of rainfall interception in forest canopies. *Ecological Modelling*, *99*(2–3), 151–159. https://doi.org/10.1016/s0304-3800(97)01948-0

Liu, S. (2001). Evaluation of the Liu model for predicting rainfall interception in forests world-wide. *Hydrological Processes*, *15*(12), 2341–2360. https://doi.org/10.1002/hyp.264

Loheide, S. P., II. (2008). A method for estimating subdaily evapotranspiration of shallow groundwater using diurnal water table fluctuations. *Ecohydrology: Ecosystems, Land and Water Process Interactions, Ecohydrogeomorphology*, *1*(1), 59–66. https://doi.org/10.1002/eco.7

Lu, J., Sun, G., McNulty, S. G., & Amatya, D. M. (2005). A comparison of six potential evapotranspiration methods for regional use in the southeastern United States 1. *JAWRA Journal of the American Water Resources Association*, *41*(3), 621–633. https://doi.org/10.1111/j.1752-1688.2005.tb03759.x

Lutz, D. A., Burakowski, E. A., Murphy, M. B., Borsuk, M. E., Niemiec, R. M., & Howarth, R. B. (2016). Trade-offs between three forest ecosystem services across the state of New Hampshire, USA: Timber, carbon, and albedo. *Ecological Applications*, *26*(1), 146–161. https://doi.org/10.1890/14-2207

Makarieva, A. M., Gorshkov, V. G., & Li, B.-L. (2013). Revisiting forest impact on atmospheric water vapor transport and precipitation. *Theoretical and Applied Climatology*, *111*(1–2), 79–96. https://doi.org/10.1007/s00704-012-0643-9

Markwitz, C., & Siebicke, L. (2019). Low-cost eddy covariance: A case study of evapotranspiration over agroforestry in Germany. *Atmospheric Measurement Techniques*, *12*(9), 4677–4696. https://doi.org/10.5194/amt-12-4677-2019

McLaughlin, D. L., & Cohen, M. J. (2011). Thermal artifacts in measurements of fine-scale water level variation. *Water Resources Research*, *47*(9), W09601. https://doi.org/10.1029/2010wr010288

McLaughlin, D. L., Kaplan, D. A., & Cohen, M. J. (2013). Managing forests for increased regional water yield in the southeastern US Coastal Plain. *Journal of the American Water Resources Association*, *49*(4), 953–965. https://doi.org/10.1111/jawr.12073

McNichol, B. H., Montes, C. R., Barnes, B. F., Nowak, J. T., Villari, C., & Gandhi, K. J. (2019). Interactions between southern Ips bark beetle outbreaks, prescribed fire, and loblolly pine (Pinus taeda L.) mortality. *Forest Ecology and Management*, *446*, 164–174. https://doi.org/10.1016/j.foreco.2019.05.036

McNulty, S. G., Archer, E. R., Gush, M. B., Van Noordwijk, M., Ellison, D., Blanco, J. A., et al. (2018). *Determinants of the forest-water relationship*. International Union of Forest Research Organizations (IUFRO).

Melo, F. P., Parry, L., Brancalion, P. H., Pinto, S. R., Freitas, J., Manhães, A. P., et al. (2021). Adding forests to the water–energy–food nexus. *Nature Sustainability*, *4*(2), 85–92. https://doi.org/10.1038/s41893-020-00608-z

Mercado-Bettín, D., Salazar, J. F., & Villegas, J. C. (2017). Global synthesis of forest cover effects on long-term water balance partitioning in large basins. *Hydrology and Earth System Sciences Discussions*, 1–18. https://doi.org/10.5194/hess-2017-550,2017

Miralles, D. G., Brutsaert, W., Dolnan, A. J., & Gash, J. H. (2020). On the use of the term "evapotranspiration". *Water Resources Research*, *56*(11), 1–5. https://doi.org/10.1029/2020wr028055

Nachabe, M., Shah, N., Ross, M., & Vomacka, J. (2005). Evapotranspiration of two vegetation covers in a shallow water table environment. *Soil Science Society of America Journal*, *69*(2), 492–499. https://doi.org/10.2136/sssaj2005.0492

Pascolini-Campbell, M., Reager, J. T., Chandanpurkar, H. A., & Rodell, M. (2021). A 10 per cent increase in global land evapotranspiration from 2003 to 2019. *Nature*, *593*(7860), 543–547. https://doi.org/10.1038/s41586-021-03503-5

Paul-Limoges, E., Wolf, S., Schneider, F. D., Longo, M., Moorcroft, P., Gharun, M., & Damm, A. (2020). Partitioning evapotranspiration with concurrent eddy covariance measurements in a mixed forest. *Agricultural and Forest Meteorology*, *280*, 107786. https://doi.org/10.1016/j.agrformet.2019.107786

Peña-Arancibia, J. L., Bruijnzeel, L. A., Mulligan, M., & van Dijk, A. I. (2019). Forests as "sponges" and "pumps": Assessing the impact of deforestation on dry-season flows across the tropics. *Journal of Hydrology*, *574*, 946–963. https://doi.org/10.1016/j.jhydrol.2019.04.064

Penman, H. L. (1948). Natural evaporation from open water, bare soil and grass. *Proceedings of the Royal Society of London - Series A: Mathematical and Physical Sciences*, *193*(1032), 120–145. https://doi.org/10.1098/rspa.1948.0037

Phelps, G. (1984). *Recharge and discharge areas of the Floridan aquifer in the St*. Johns River Water Management District and vicinity.

Pypker, T. G., Bond, B. J., Link, T. E., Marks, D., & Unsworth, M. H. (2005). The importance of canopy structure in controlling the interception loss of rainfall: Examples from a young and an old-growth Douglas-fir forest. *Agricultural and Forest Meteorology*, *130*(1–2), 113–129. https://doi.org/10.1016/j.agrformet.2005.03.003

Rothacher, J. (1970). Increases in water yield following clear-cut logging in the Pacific Northwest. *Water Resources Research*, *6*(2), 653–658. https://doi.org/10.1029/wr006i002p00653

Sahin, V., & Hall, M. J. (1996). The effects of afforestation and deforestation on water yields. *Journal of hydrology*, *178*(1–4), 293–309. https://doi.org/10.1016/0022-1694(95)02825-0

Samuelson, L. J., Stokes, T. A., Butnor, J. R., Johnsen, K. H., Gonzalez-Benecke, C. A., Martin, T. A., et al. (2017). Ecosystem carbon density and allocation across a chronosequence of longleaf pine forests. *Ecological Applications*, *27*(1), 244–259. https://doi.org/10.1002/eap.1439

Savenije, H. H. (2004). The importance of interception and why we should delete the term evapotranspiration from our vocabulary. *Hydrological Processes*, *18*(8), 1507–1511. https://doi.org/10.1002/hyp.5563

Schenk, H. J., & Jackson, R. B. (2002). The global biogeography of roots. *Ecological Monographs*, *72*(3), 311–328. https://doi.org/10.1890/0012-9615

Schulze, R., & George, W. (1987). A dynamic, process-based, user-oriented model of forest effects on water yield. *Hydrological Processes*, *1*(3), 293–307. https://doi.org/10.1002/hyp.3360010308

Schwaiger, F., Poschenrieder, W., Biber, P., & Pretzsch, H. (2019). Ecosystem service trade-offs for adaptive forest management. *Ecosystem Services*, *39*, 100993. https://doi.org/10.1016/j.ecoser.2019.100993

Shoemaker, W. B., & Sumner, D. M. (2006). Alternate corrections for estimating actual wetland evapotranspiration from potential evapotranspiration. *Wetlands*, *26*(2), 528–543. https://doi.org/10.1672/0277-5212(2006)26[528:acfeaw]2.0.co;2

Singh, B., & Szeicz, G. (1979). The effect of intercepted rainfall on the water balance of a hardwood forest. *Water Resources Research*, *15*(1), 131–138. https://doi.org/10.1029/wr015i001p00131

Sohngen, B., Mendelsohn, R., & Sedjo, R. (1999). Forest management, conservation, and global timber markets. *American Journal of Agricultural Economics*, *81*(1), 1–13. https://doi.org/10.2307/1244446

Soubie, R., Heinesch, B., Granier, A., Aubinet, M., & Vincke, C. (2016). Evapotranspiration assessment of a mixed temperate forest by four methods: Eddy covariance, soil water budget, analytical and model. *Agricultural and Forest Meteorology*, *228*, 191–204. https://doi.org/10.1016/j.agrformet.2016.07.001

Stednick, J. D. (1996). Monitoring the effects of timber harvest on annual water yield. *Journal of hydrology*, *176*(1–4), 79–95. https://doi.org/10.1016/0022-1694(95)02780-7

Stenberg, P., Linder, S., Smolander, H., & Flower-Ellis, J. (1994). Performance of the LAI-2000 plant canopy analyzer in estimating leaf area index of some Scots pine stands. *Tree Physiology*, *14*(7–8-9), 981–995. https://doi.org/10.1093/treephys/14.7-8-9.981

Stephens, S. L., Agee, J. K., Fule, P. Z., North, M., Romme, W., Swetnam, T., & Turner, M. G. (2013). Managing forests and fire in changing climates. *Science*, *342*(6154), 41–42. https://doi.org/10.1126/science.1240294

Stickler, C. M., Coe, M. T., Costa, M. H., Nepstad, D. C., McGrath, D. G., Dias, L. C., et al. (2013). Dependence of hydropower energy generation on forests in the Amazon Basin at local and regional scales. *Proceedings of the National Academy of Sciences*, *110*(23), 9601–9606. https://doi.org/10.1073/pnas.1215331110

Sun, G. (2013). Impacts of climate change and variability on water resources in the Southeast USA. In *Climate of the southeast United States* (pp. 210–236). Springer.

Sun, G., Alstad, K., Chen, J., Chen, S., Ford, C. R., Lin, G., et al. (2011). A general predictive model for estimating monthly ecosystem evapotranspiration. *Ecohydrology*, *4*(2), 245–255. https://doi.org/10.1002/eco.194

Sun, G., Caldwell, P., Noormets, A., McNulty, S. G., Cohen, E., Moore Myers, J., et al. (2011). Upscaling key ecosystem functions across the conterminous United States by a water-centric ecosystem model. *Journal of Geophysical Research*, *116*(G3), G00J05. https://doi.org/10.1029/2010jg001573

Sun, G., McNulty, S. G., Moore Myers, J. A., & Cohen, E. C. (2008). Impacts of multiple stresses on water demand and supply across the Southeastern United States 1. *JAWRA Journal of the American Water Resources Association*, *44*(6), 1441–1457. https://doi.org/10.1111/j.1752-1688.2008.00250.x

Sun, G., Noormets, A., Chen, J., & McNulty, S. (2008). Evapotranspiration estimates from eddy covariance towers and hydrologic modeling in managed forests in Northern Wisconsin, USA. *Agricultural and Forest Meteorology*, *148*(2), 257–267. https://doi.org/10.1016/j.agrformet.2007.08.010

Sun, G., Riekerk, H., & Comerford, N. B. (1998). Modeling the forest hydrology of wetland-upland ecosystems in Florida 1. *JAWRA Journal of the American Water Resources Association*, *34*(4), 827–841. https://doi.org/10.1111/j.1752-1688.1998.tb01519.x

Sun, G., Zuo, C., Liu, S., Liu, M., McNulty, S. G., & Vose, J. M. (2008). Watershed evapotranspiration increased due to changes in vegetation composition and structure under a subtropical climate 1. *Jawra Journal of the American Water Resources Association*, *44*(5), 1164–1175. https://doi.org/10.1111/j.1752-1688.2008.00241.x

Susaeta, A., Adams, D. C., Gonzalez-Benecke, C., & Soto, J. R. (2017). Economic feasibility of managing loblolly pine forests for water production under climate change in the Southeastern United States. *Forests*, *8*(3), 83. https://doi.org/10.3390/f8030083

Susaeta, A., Soto, J. R., Adams, D. C., & Allen, D. L. (2016). Economic sustainability of payments for water yield in slash pine plantations in Florida. *Water*, *8*(9), 382. https://doi.org/10.3390/w8090382

Team, R. C. (2020). *R: A language and environment for statistical computing. Version 4.0.2*.

Trømborg, E., Buongiorno, J., & Solberg, B. (2000). The global timber market: Implications of changes in economic growth, timber supply, and technological trends. *Forest Policy and Economics*, *1*(1), 53–69. https://doi.org/10.1016/s1389-9341(00)00005-8

Tuanmu, M. N., Viña, A., Yang, W., Chen, X., Shortridge, A. M., & Liu, J. (2016). Effects of payments for ecosystem services on wildlife habitat recovery. *Conservation Biology*, *30*(4), 827–835. https://doi.org/10.1111/cobi.12669

Van Laar, A., & Akça, A. (2007). *Forest mensuration*. Springer Science & Business Media.

Van Rees, K. C., & Comerford, N. B. (1986). Vertical root distribution and strontium uptake of a slash pine stand on a Florida Spodosol. *Forest and Range Soil*, *50*(4), 1042–1046. https://doi.org/10.2136/sssaj1986

Vose, J. M., Dougherty, P. M., Long, J. N., Smith, F. W., Gholz, H. L., & Curran, P. J. (1994). Factors influencing the amount and distribution of leaf area of pine stands. *Ecological Bulletins*, *43*, 102–114.

Wang, Q., Adiku, S., Tenhunen, J., & Granier, A. (2005). On the relationship of NDVI with leaf area index in a deciduous forest site. *Remote Sensing of Environment*, *94*(2), 244–255. https://doi.org/10.1016/j.rse.2004.10.006

Wang, W., Dwivedi, P., Abt, R., & Khanna, M. (2015). Carbon savings with transatlantic trade in pellets: Accounting for market-driven effects. *Environmental Research Letters*, *10*(11), 114019. https://doi.org/10.1088/1748-9326/10/11/114019

Weiss, M., Baret, F., Smith, G., Jonckheere, I., & Coppin, P. (2004). Review of methods for in situ leaf area index (LAI) determination: Part II. Estimation of LAI, errors and sampling. *Agricultural and Forest Meteorology*, *121*(1–2), 37–53. https://doi.org/10.1016/j.agrformet.2003.08.001

Wetzel, P. J., & Chang, J.-T. (1987). Concerning the relationship between evapotranspiration and soil moisture. *Journal of Applied Meteorology and Climatology*, *26*(1), 18–27. https://doi.org/10.1175/1520-0450(1987)026<0018:ctrbea>2.0.co;2

White, W. N. (1932). *A method of estimating ground-water supplies based on discharge by plants and evaporation from soil: Results of investigations in Escalante Valley*. US Government Printing Office.

Willaarts, B. (2012). *Linking land management to water planning: Estimating the water consumption of Spanish forests, water, agriculture and the environment in Spain: Can we square the circle* (pp. 139–151).

Yurtseven, I., Serengil, Y., Gökbulak, F., Şengönül, K., Ozhan, S., Kılıç, U., et al. (2018). Results of a paired catchment analysis of forest thinning in Turkey in relation to forest management options. *The Science of the Total Environment*, *618*, 785–792. https://doi.org/10.1016/j.scitotenv.2017.08.190

Zhang, M., Liu, N., Harper, R., Li, Q., Liu, K., Wei, X., et al. (2017). A global review on hydrological responses to forest change across multiple spatial scales: Importance of scale, climate, forest type and hydrological regime. *Journal of Hydrology*, *546*, 44–59. https://doi.org/10.1016/j.jhydrol.2016.12.040

Zwick, P. D., & Carr, M. H. (2006). *Florida 2060: A population distribution scenario for the state of Florida*. Report to. (p. 1000).